Sciencexpress Reports

Dynamics of DNA Supercoils

M. T. J. van Loenhout, M. V. de Grunt, C. Dekker*

Delft University of Technology, Department of Bionanoscience, Kavli Institute of Nanoscience, Lorentzweg 1, 2628CJ Delft, Netherlands.

*To whom correspondence should be addressed. E-mail: c.dekker@tudelft.nl

DNA in cells exhibits a supercoiled state where the double helix is additionally twisted to form extended intertwined loops called plectonemes. Although supercoiling is vital to many cellular processes, its dynamics remain elusive. Here we directly visualize the dynamics of individual plectonemes. We observe that multiple plectonemes can be present and that their number depends on applied stretching force and ionic strength. Plectonemes moved along DNA by diffusion or, unexpectedly, by a fast hopping process that facilitated very rapid (<20 ms) long-range plectoneme displacement by nucleating a new plectoneme at a distant position. The observations directly reveal the dynamics of plectonemes and identify a new mode of movement that allows long-distance reorganization of the conformation of the genome on a millisecond time scale.

Supercoiling and changes in the supercoiling state are ubiquitous in cellular DNA and affect virtually all genomic processes (*1*). Proteins moving along the helical path of the DNA, for example, generate torsional stress, which produces twist (the over- or under-winding of the DNA double helix around its axis) and writhe (the coiling of the duplex axis around itself). Supercoiling affects the cell because it alters the conformation of the genome on two basic levels. First, supercoiling can induce local changes in the DNA structure such as a locally destabilized or deformed duplex, which subsequently affect transcription or trigger protein binding (*2*–*4*). Second, supercoiling can induce global changes in the conformation of the genome, which brings distant DNA sequences together thereby facilitating DNA compaction and site-specific recombination (*5*, *6*). Genomic DNA is organized in topological domains of 10-100 kilobases (kb) which isolate topological changes from neighboring regions (*1*). Within these regions, torsion can rapidly transmit allowing for long-range communication between distant genomic locations (*7*). To understand the cellular processes that are affected by supercoiling, it is essential to know its dynamics, of which virtually nothing is known. Do plectonemes move along DNA, and if so, by which process, and on what time scale? We address these questions at the single-molecule level.

The dynamics of supercoiled DNA has been difficult to address experimentally. Static images obtained by electron and atomic force microscopy showed that supercoiled plasmids are plectonemic (*8*, *9*). These images could not capture the dynamics as DNA needs to be strongly immobilized for imaging. Measurements of site-specific recombination have provided indirect information on the speed of juxtaposition of DNA positions, but these results did not agree with theoretical predictions, leaving many unanswered questions on the dynamics on the diffusion speed of plectonemes (*6*, *10*). Single-molecule magnetic tweezers have proven to be an ideal platform to study DNA mechanics as they allow to twist and apply a stretching force to a single DNA molecule (*11*). In the traditional implementation this technique is limited, however, as it only measures the DNA end-to-end distance and not the position of a plectoneme along the DNA tether.

To visualize the dynamics of plectonemes directly along a single DNA molecule, we developed a magnetic tweezers apparatus (Fig. 1A) that pulls a fluorescently labeled DNA molecule sideways and visualizes it along its length using epi-fluorescence. Each experiment started by creating plectonemes in a DNA molecule that was torsionally constrained between the flow cell surface and a magnetic bead by coiling it with a pair of magnets positioned above the DNA tether. The DNA molecule was positively supercoiled to a degree where 25% of the DNA contour length was put into a plectonemic state (Fig. 1B and table S1). Subsequently, an additional magnet was brought near to side of the flow cell and the top magnets were removed, thereby pulling the DNA tether sideways at modest stretching forces (0.4-3.2 pN), which are readily generated by, for example polymerases in vivo (*12*). All measurements were performed on 21-kb DNA molecules, similar in length to the topological domains observed in genomic DNA (*1*). The DNA molecules were covalently labeled with Cy3 dyes attached by a long (~3 nm) linker at random positions along their length resulting in a low labeling density of ~1/25 bp. An efficient oxygen scavenging system (*13*) allowed us to monitor supercoiled DNA molecules for several seconds before photo-induced nicking occurs, which released all torsional stress. Cy3 labeling did not affect the mechanical properties of the DNA, as shown by the rotation curves of labeled molecules which overlap with those of unlabeled molecules (Fig. 1B and fig. S1) (*14*).

We observed individual plectonemes in supercoiled DNA molecules in images acquired with 20-ms time resolution. As illustrated in Fig. 1C and movie S1 (*14*), plectonemes appear in the images as bright spots along the DNA, as the local DNA density is higher in the plectonemes. These bright spots were near-diffraction-limited with a typical spot size of ~500 nm. The spots were not present in non-supercoiled DNA and disappeared instantly if a DNA molecule became nicked (fig. S2) (*14*).

We observed that multiple plectonemes were present that appeared and disappeared and that moved along the DNA. The dynamics of plectonemes were analyzed by converting the time series of images to kymographs, which plot the intensity profile along the DNA position versus time (Fig. 1D). Within the 2-s time scale of the kymograph in Fig. 1D, we observed many events where plectonemes nucleated, moved, and disappeared some time later. A fitting routine was developed to count and extract their position over time (figs. S3 to S5) (*14*). A typical result is shown in Fig. 1E where individual plectonemes are marked by colored lines.

We find that the number of plectonemes in the DNA varies substantially with ionic strength and applied force. Experiments were performed for a range of ionic strengths ([NaCl] = 20 to 300 mM) and forces (f = 0.4 to 3.2 pN) (Fig. 2A and movie S2) (*14*). Plectonemes were found to be very dynamic at low forces and quickly moved between positions along the DNA. At higher forces, the dynamics become restricted and single plectonemes remain at the same position for long periods in time (several seconds), giving rise to almost static high intensity bands in the kymographs. The number of plectonemes present at any given time varied from a single one for high-force and high-salt conditions to about three for low-force and low-salt conditions (Fig. 2, B and C). The mean size of individual plectonemes varied between ~1.7 and ~5.3 kb, which is consistent with the ~2.3 kb observed by electron microscopy (*8*) and predictions of Monte Carlo simulations (*15*). Our results confirm the general trends described in two recent theoretical studies by Emanuel *et al*. (*16*) and Marko *et al*. (*17*), which predict the presence of multiple plectonemes for low force (<0.5 pN), or low salt concentrations (<50

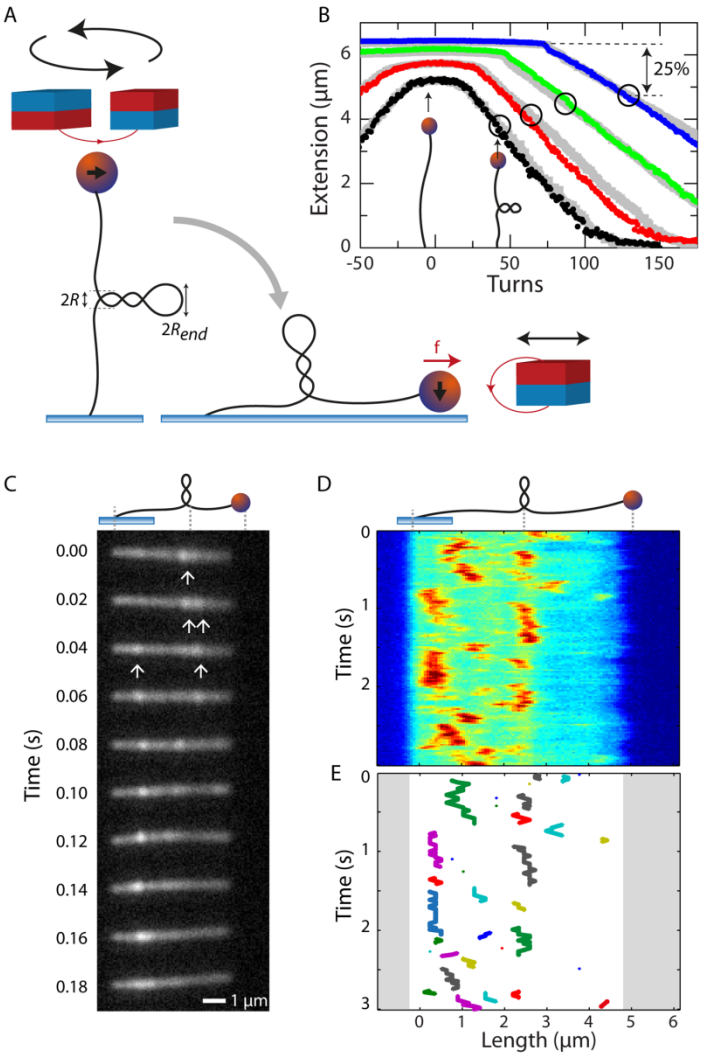

Fig. 1. Visualization of plectonemes by fluorescence with side-pulling magnetic tweezers. (**A**) A DNA molecule is supercoiled by rotating a pair of magnets and is subsequently pulled sideways with an additional magnet into the focal plane of a high numerical aperture objective. (**B**) DNA rotation curves of a Cy3-labeled 21 kb molecule in a 300 mM NaCl buffer at various forces (black to blue: 0.4, 0.8, 1.6. 3.2 pN) and a non-labeled molecule (gray points). Experiments were performed at conditions where 25% of the DNA contour length was put in a plectonemic state (open circles). (**C**) Images at consecutive 20 ms intervals of a supercoiled DNA molecule showing plectonemes (arrows) at a force of 0.8 pN in a buffer containing 150 mM NaCl. (**D**) Kymograph of the supercoiled DNA molecule shown in panel (D) constructed by summation of the pixel intensities perpendicular to the stretching direction of the molecule, plotting the intensity (color scale) versus position and time. Plectonemes are visible as high-intensity regions in the kymograph. (**E**) Same kymograph as in panel (D) after background subtraction and peak fitting (figs. S3 to S5). Individual plectonemes identified in consecutive frames are indicated with different colors.

mM). At higher forces and increased salt concentrations (≥1 pN, >50 mM) Marko *et al*. (*17*) predict the presence of only a single plectonemic domain in a 10 kb DNA molecule, whereas we observed that a few plectonemes could still be present under these conditions.

The number of plectonemes present in a DNA molecule will be set by the free energy balance between the change in enthalpy and the change in entropy upon the formation of an additional plectoneme (*15*). Entropy will favor the presence of multiple plectonemes as they can occupy multiple positions along the molecule and distribute the writhe between them (*16*, *17*). The energy cost required to bend the DNA in the plectoneme, however, will favor a single plectoneme. The structure of a plectoneme can be simplified to consist of an intertwined section and an end loop (Fig. 1A). The formation of an end loop with size $2R_{end}$ is energetically more costly than extending the intertwined region, making it unfavorable to form multiple plectonemes (*18*). Surprisingly, the data showed that multiple plectonemes were present in DNA molecules.

The observed number of plectonemes decreased for higher ionic strengths (Fig. 2, B and C), which may be understood by considering the plectoneme structure. Increasing ionic strength will screen the electrostatic repulsion between the highly charged DNA backbones and leads to a reduction of the plectoneme radius (R) compared to the end loop radius (R_{end}) which is set by the mechanical bending of the DNA (*19*, *20*). At high ionic strength, $R < R_{end}$ which favors a single plectoneme, but at low ionic strength R increases and becomes approximately equal to R_{end}, reducing the free energy penalty for forming additional plectonemes. Indeed, this response was experimentally observed as the number of plectonemes increased with decreasing ionic strength (Fig. 2, B and C). The applied stretching force did not have a strong influence on the number of plectonemes (Fig. 2B). In contrast to ionic strength, an applied stretching force would reduce both R and R_{end} making the free energy penalty for the formation of an additional plectoneme rather insensitive to force.

We now turn to the dynamics of plectonemes. Here, unexpectedly, we observed two different types of motion. First, diffusive motion where a plectoneme randomly moved along a DNA molecule (Fig. 3, A to C). Second, hopping where a plectoneme suddenly shrank or disappeared while simultaneously a new plectoneme nucleated at a different location (Fig. 4, A to C). We first focus on diffusion. To quantify the diffusive behavior of plectonemes, we tracked the position of individual plectonemes with an extended lifetime (≥0.3 s) (Fig. 3B and fig. S6)

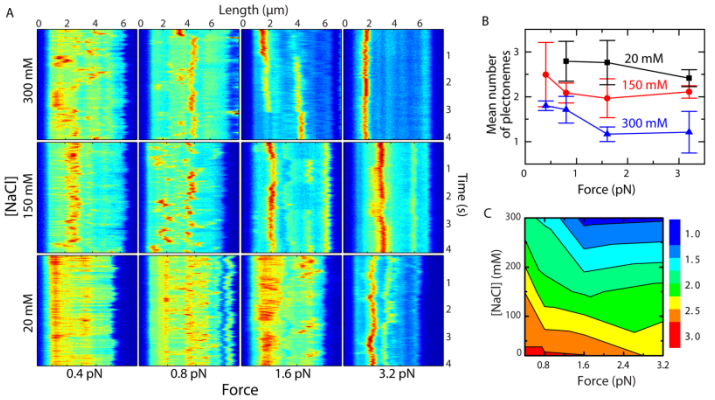

Fig. 2. The number of plectonemes and their dynamics depend on the applied stretching force and ionic strength. (**A**) Kymographs of DNA molecules for 12 different stretching force/ionic strength combinations (also available as movie S2). (**B**) The mean number of plectonemes increases with decreasing ionic strength ($n \geq 4$ DNA molecules per data point, error bars indicate the standard deviation. (**C**) Phase diagram showing the dependence of the number of plectonemes on applied stretching force and ionic strength.

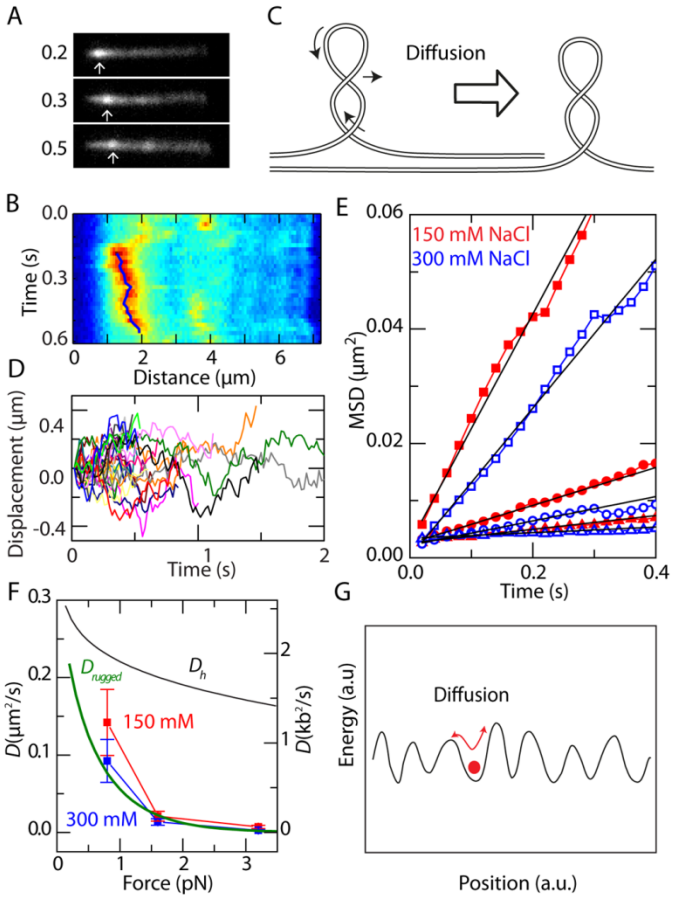

Fig. 3. Plectoneme diffusion along a DNA molecule. (**A**) Images and (**B**) kymograph of a plectoneme diffusing along a DNA molecule (150 mM NaCl, 0.8 pN). Solid line denotes the diffusional track of the plectoneme as obtained by a fit to the intensity in the kymograph (blue line, fig. S6). (**C**) Diffusion of a plectoneme involves the sideways movement of the DNA but also a slithering motion within the plectoneme. (**D**) Example of diffusion traces. (**E**) Mean squared displacement (MSD) of plectoneme positions at 0.8 pN (squares), 1.6 pN (circles), and 3.2 pN (triangles) stretching force. Lines are linear fits to the MSD (supplementary text S1). (**F**) Diffusion constants, corrected for the DNA extension at the experimentally probed forces (supplementary text S1), obtained from linear fits of panel (E). The observed diffusion constants decrease are much lower than those predicted from a hydrodynamic diffusion model (black line, supplementary text S3). A model incorporating a rugged energy landscape (green line, fig. S7) fits the 300 mM data well. (**G**) Schematic diagram of plectoneme diffusion in a rugged energy landscape along a DNA molecule.

(*14*). An example of the diffusional tracks for 24 plectonemes is shown in Fig. 3D. To extract the plectoneme diffusion constant (D), we calculated the mean squared displacement (MSD), $\langle \Delta x^2(t) \rangle$, where Δx is the plectoneme displacement along the DNA and $\langle\ \rangle$ denotes the time average (supplementary text S1 and S2) (*14*). As Fig. 3E shows, we observe a near-linear relation of the MSD with time, $\langle \Delta x^2(t) \rangle = 2Dt$, which is characteristic for Brownian motion, indicating that plectonemes indeed move along DNA by one-dimensional diffusion, similar to the diffusion of knots in DNA (*21*).

Diffusion of a plectoneme requires not only the sideways motion of the plectoneme, but also the slithering motion of the DNA within the supercoil (Fig. 3C) (*22*). Remarkably, the diffusional constants that were experimentally observed were substantially lower than those predicted for the hydrodynamic drag of plectonemes (Fig. 3F and supplementary text S3) (*14*) and showed a rapid decrease with applied stretching force (Fig. 3, E and F). Surface effects caused by the proximity of the DNA molecule to the surface cannot explain such a large reduction in diffusion speed as they result only in a very small increase in the viscous drag (supplementary text S4) (*14*).

The unexpectedly slow diffusion of plectonemes can originate from different microscopic causes, which in there most general form, may be represented by the presence of a rugged energy landscape that the plectoneme must navigate while moving along the DNA molecule. This energy landscape can derive from sequence-dependent mechanical properties such as the intrinsic curvature and bendability of the DNA that create local energy barriers for diffusion (*23*). Indeed, we observed that plectonemes are not fully randomly distributed along a DNA molecule, but have some preference for certain positions along the DNA (Fig. 2A).

We can quantitatively estimate the effect of a rugged energy potential on the diffusive motion of a plectoneme by expressing the actual diffusion constant D as the product of the hydrodynamic diffusion constant D_h and a retardation factor $F(\varepsilon)$. If we assume that the fluctuating part of the potential energy landscape along the DNA molecule obeys a Gaussian distribution, then $F(\varepsilon) = \exp[-(\varepsilon/k_BT)^2]$, where ε denotes the root-mean-square (rms) fluctuations in the energy potential (*24*). As the bending energy for looping DNA scales as the square root of the applied stretching force (*25*), we propose a rugged-energy model with $\varepsilon(f) \propto \sqrt{f}$. Indeed, this provides an excellent fit (green line Fig. 3F) to the experimental data compared to the simple hydrodynamic model (black line in Fig. 3F; fig. S7) (*14*). We found values for ε of 1 k_BT at 150 mM and 0.8 pN to 2 k_BT at 300 mM and 3.2 pN, which represent only a small modulation compared to the bending energies of the end loop which are 14 and 28 k_BT respectively (*25*). Importantly, the values of ε are close to the thermal energy, allowing for diffusion to occur, albeit at a reduced speed.

The second mechanism whereby plectonemes moved along DNA is hopping, where one plectoneme suddenly shrank or vanished and a new one simultaneously nucleated at a different position along the DNA (Fig. 4, A to C). These hopping events were generally fast, occurring abruptly within the 20 ms of our single-frame time resolution, and spanned large distances that could not be explained by a diffusion mechanism (Fig. 4, A and B, and supplementary text S5) (*14*). The total length of DNA in plectonemes was constant at 25% in our experiments, so shrinking of a plectoneme necessarily resulted in the growing or nucleation of a new plectoneme and the observed nucleation rate (0.3-22 s^{-1}) is equivalent to the hopping rate. This rate decreased with increasing force and ionic strength (*18*) (Fig. 4D and supplementary text S6) (*14*), while the mean plectoneme lifetime (0.1-10 s) increased strongly with force and ionic strength (Fig. 4E). The distribution of plectoneme lifetimes showed a strong decrease with time (Fig. 4F), i.e., most plectonemes are short lived (<0.1 s).

We can explain the distribution of lifetimes by considering what happens after nucleation of a plectoneme. It can either grow by absorbing more writhe, or shrink by releasing writhe. The growing and shrinking of a plectoneme can be described by a random walk, and the lifetime of the plectoneme is then set by the first return to the origin of the walk, i.e., the nucleation point. The probability of this first return at time t is

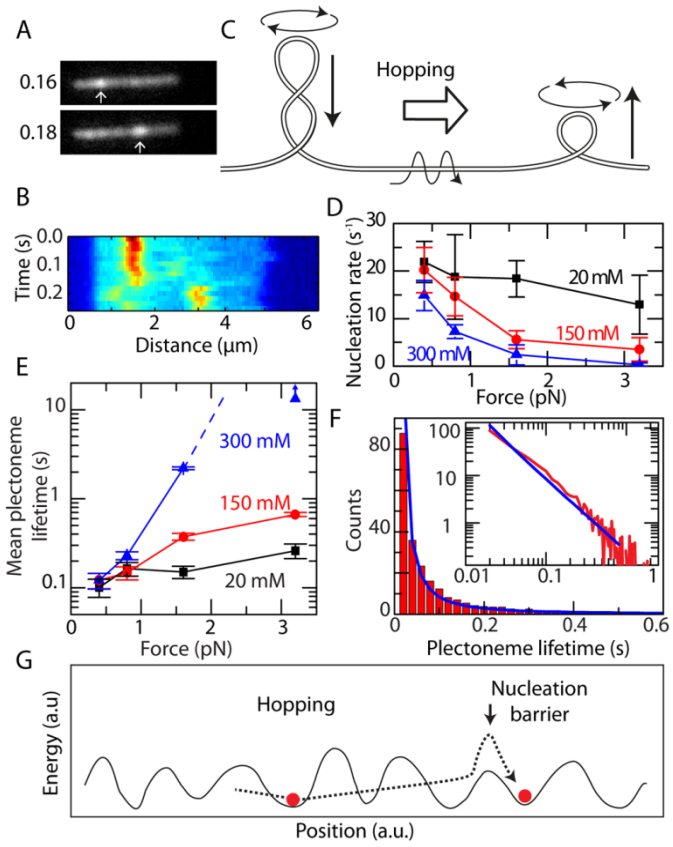

Fig. 4. Plectoneme hopping along a DNA molecule. (**A**) Images and (**B**) kymograph of a hopping event (150 mM NaCl, 0.8 pN). (**C**) Hopping of a plectoneme involves the nucleation of a new loop at a different location and the transfer of writhe by rotation and sideways motion of the intermediate DNA. (**D**) Nucleation rate of plectonemes as a function of force at different ionic strengths (supplementary text S6, $n \geq 4$ DNA molecules for each condition; error bars indicate the standard deviation). (**E**) Mean plectoneme lifetime versus force ($n \geq 4$ DNA molecules for each condition; error bars indicate the standard deviation, the data point at 3.2 pN, 300 mM NaCl only provides a lower bound as nicking of the DNA molecule limited the observed lifetimes). (**F**) Histogram of the plectoneme lifetimes at 150 mM NaCl, 0.8 pN; inset shows the same data on a loglog scale. A model for the first-return-to-the-origin of a random walk for the same number of events agrees well with the experimental data (blue lines). (**G**) Schematic diagram showing that hopping can bypass roughness in the energy landscape that retards diffusion along the molecule.

given by $P(t)=\binom{t}{t/2}(t-1)2^{-t}$, where $\binom{t}{t/2}$ denotes the binomial coefficient. Indeed, this random-walk model described the experimental data well (blue lines in Fig. 4F; supplementary text S7) (*14*). A similar scaling of the lifetimes was observed for all experimental conditions (fig. S8) (*14*).

Hopping allows plectonemes to move over large distances. We observed maximum hopping distances of up to 15 kb (~5 μm) in our 21-kb DNA molecules (fig. S9) (*14*). Interestingly, hopping can occur over these large distances irrespective of the rugged energy landscape in between, as the nucleation at the new location is independent of any energy barriers associated with the DNA in between the shrinking plectoneme and the nucleation spot (Fig. 4G). Hopping is merely restricted by the energy required for nucleation of a new plectoneme and the subsequent transfer of writhe to the new plectoneme by the rotation of the intermediate DNA. The nucleation barrier depends both on applied stretching force and ionic strength, predicting lower nucleation rates at high force and high ionic strength (*18*), which is indeed the behavior we observe (Fig. 4D).

The viscous drag associated with the rotation and movement of the intermediate DNA during hopping (Fig. 4C) grew only slowly with distance and was much smaller than the drag for the diffusion of a plectoneme. Surprisingly, thermal fluctuations led to a hopping distance that scaled linearly with time, in contrast to the distance for diffusive motion, which scaled as the square root of time (supplementary text S8) (*14*). The lower drag allowed plectonemes to relocate by hopping over many kilobases in a fraction of a second, which would be impossible for diffusion of a plectoneme along the DNA molecule.

The observed dynamics of DNA supercoils reveal how plectonemes change the DNA conformation. Multiple plectonemes were found to be present in a supercoiled DNA molecule under applied force, with a typical density of 1 plectoneme per 10 kb. Diffusion of plectonemes was strongly dependent on applied stretching force, suggesting that it is retarded by local inhomogeneities in the DNA mechanical properties. In contrast, hopping of plectonemes results in a fast long-range rearrangement of the DNA conformation, which may explain the fast search times for site juxtaposition of two distant DNA regions. Hopping can also aid to recruit a plectoneme to a DNA sequence that exhibits inherent curvature or to a site of protein-induced DNA bending. Such a mechanism will allow to change the conformation of the genome at millisecond timescale, thereby triggering protein binding or influencing gene expression.

References and Notes

1. J. Roca, The torsional state of DNA within the chromosome. *Chromosoma* **120**, 323 (2011). doi:10.1007/s00412-011-0324-y Medline
2. I. De Vlaminck *et al*., Torsional regulation of hRPA-induced unwinding of double-stranded DNA. *Nucleic Acids Res.* **38**, 4133 (2010). doi:10.1093/nar/gkq067 Medline
3. L. F. Liu, J. C. Wang, Supercoiling of the DNA template during transcription. *Proc. Natl. Acad. Sci. U.S.A.* **84**, 7024 (1987). doi:10.1073/pnas.84.20.7024 Medline
4. M. R. Gartenberg, J. C. Wang, Positive supercoiling of DNA greatly diminishes mRNA synthesis in yeast. *Proc. Natl. Acad. Sci. U.S.A.* **89**, 11461 (1992). doi:10.1073/pnas.89.23.11461 Medline
5. K. Kimura, T. Hirano, ATP-dependent positive supercoiling of DNA by 13S condensin: A biochemical implication for chromosome condensation. *Cell* **90**, 625 (1997). doi:10.1016/S0092-8674(00)80524-3 Medline
6. C. N. Parker, S. E. Halford, Dynamics of long-range interactions on DNA: The speed of synapsis during site-specific recombination by resolvase. *Cell* **66**, 781 (1991). doi:10.1016/0092-8674(91)90121-E Medline
7. F. Kouzine, S. Sanford, Z. Elisha-Feil, D. Levens, The functional response of upstream DNA to dynamic supercoiling in vivo. *Nat. Struct. Mol. Biol.* **15**, 146 (2008). doi:10.1038/nsmb.1372 Medline
8. T. C. Boles, J. H. White, N. R. Cozzarelli, Structure of plectonemically supercoiled DNA. *J. Mol. Biol.* **213**, 931 (1990). doi:10.1016/S0022-2836(05)80272-4 Medline
9. G. Zuccheri, R. T. Dame, M. Aquila, I. Muzzalupo, B. Samori, Conformational fluctuations of supercoiled DNA molecules observed in real time with a scanning force microscope. *Appl. Phys. A Mater. Sci. Process.* **66**, S585 (1998). doi:10.1007/s003390051206
10. M. Oram, J. F. Marko, S. E. Halford, Communications between distant sites on supercoiled DNA from non-exponential kinetics for DNA synapsis by resolvase. *J. Mol. Biol.* **270**, 396 (1997). doi:10.1006/jmbi.1997.1109 Medline

11. T. R. Strick, J.-F. Allemand, D. Bensimon, A. Bensimon, V. Croquette, The elasticity of a single supercoiled DNA molecule. *Science* **271**, 1835 (1996). doi:10.1126/science.271.5257.1835 Medline
12. M. D. Wang *et al*., Force and velocity measured for single molecules of RNA polymerase. *Science* **282**, 902 (1998). doi:10.1126/science.282.5390.902 Medline
13. C. E. Aitken, R. A. Marshall, J. D. Puglisi, An oxygen scavenging system for improvement of dye stability in single-molecule fluorescence experiments. *Biophys. J.* **94**, 1826 (2008). doi:10.1529/biophysj.107.117689 Medline
14. Materials and methods are available as supplementary materials on *Science* Online.
15. A. V. Vologodskii, S. D. Levene, K. V. Klenin, M. Frank-Kamenetskii, N. R. Cozzarelli, Conformational and thermodynamic properties of supercoiled DNA. *J. Mol. Biol.* **227**, 1224 (1992). doi:10.1016/0022-2836(92)90533-P Medline
16. M. Emanuel, G. Lanzani, H. Schiessel, Multi-plectoneme phase of double-stranded DNA under torsion. http://arxiv.org/abs/1204.1324v2 (2012).
17. J. F. Marko, S. Neukirch, Competition between curls and plectonemes near the buckling transition of stretched supercoiled DNA. *Phys. Rev. E* **85**, 011908 (2012). doi:10.1103/PhysRevE.85.011908 Medline
18. H. Brutzer, N. Luzzietti, D. Klaue, R. Seidel, Energetics at the DNA supercoiling transition. *Biophys. J.* **98**, 1267 (2010). doi:10.1016/j.bpj.2009.12.4292 Medline
19. D. Stigter, Interactions of highly charged colloidal cylinders with applications to double-stranded DNA. *Biopolymers* **16**, 1435 (1977). doi:10.1002/bip.1977.360160705 Medline
20. S. Neukirch, J. F. Marko, Analytical description of extension, torque, and supercoiling radius of a stretched twisted DNA. *Phys. Rev. Lett.* **106**, 138104 (2011). doi:10.1103/PhysRevLett.106.138104 Medline
21. X. R. Bao, H. J. Lee, S. R. Quake, Behavior of complex knots in single DNA molecules. *Phys. Rev. Lett.* **91**, 265506 (2003). doi:10.1103/PhysRevLett.91.265506 Medline
22. J. F. Marko, E. D. Siggia, Fluctuations and supercoiling of DNA. *Science* **265**, 506 (1994). doi:10.1126/science.8036491 Medline
23. C. H. Laundon, J. D. Griffith, Curved helix segments can uniquely orient the topology of supertwisted DNA. *Cell* **52**, 545 (1988). doi:10.1016/0092-8674(88)90467-9 Medline
24. R. Zwanzig, Diffusion in a rough potential. *Proc. Natl. Acad. Sci. U.S.A.* **85**, 2029 (1988). doi:10.1073/pnas.85.7.2029 Medline
25. T. R. Strick *et al*., Stretching of macromolecules and proteins. *Rep. Prog. Phys.* **66**, 1 (2003). doi:10.1088/0034-4885/66/1/201
26. P. S. Slattum *et al*., Efficient in vitro and in vivo expression of covalently modified plasmid DNA. *Mol. Ther.* **8**, 255 (2003). doi:10.1016/S1525-0016(03)00152-7 Medline
27. A. Revyakin, R. H. Ebright, T. R. Strick, Single-molecule DNA nanomanipulation: improved resolution through use of shorter DNA fragments. *Nat. Methods* **2**, 127 (2005). doi:10.1038/nmeth0205-127 Medline
28. H. Qian, M. P. Sheetz, E. L. Elson, Single particle tracking. Analysis of diffusion and flow in two-dimensional systems. *Biophys. J.* **60**, 910 (1991). doi:10.1016/S0006-3495(91)82125-7 Medline
29. J. D. Moroz, P. Nelson, Entropic elasticity of twist-storing polymers. *Macromolecules* **31**, 6333 (1998). doi:10.1021/ma971804a
30. I. De Vlaminck, C. Dekker, Recent advances in magnetic tweezers. *Annu. Rev. Biophys.* **41**, 453 (2012). doi:10.1146/annurev-biophys-122311-100544 Medline
31. F. Gittes, C. F. Schmidt, Thermal noise limitations on micromechanical experiments. *Eur. Biophys. J.* **27**, 75 (1998). doi:10.1007/s002490050113
32. S. Broersma, Viscous force constant for a closed cylinder. *J. Chem. Phys.* **32**, 1632 (1960). doi:10.1063/1.1730995
33. D. Stigter, The charged colloidal cylinder with a gouy double layer. *J. Colloid Interface Sci.* **53**, 296 (1975). doi:10.1016/0021-9797(75)90016-8
34. J. F. Marko, E. D. Siggia, Stretching DNA. *Macromolecules* **28**, 8759 (1995). doi:10.1021/ma00130a008
35. Y. Takaisi, The forces on a circular cylinder moving with low speeds in a semi-infinite viscous liquid bounded by a plane wall. *J. Phys. Soc. Jpn.* **10**, 407 (1955). doi:10.1143/JPSJ.10.407
36. C. M. Grinstead, J. L. Snell, *Introduction to Probability* (American Mathematical Society, Hanover, NH, ed. 2, 1997).
37. D. Sornette, *Critical Phenomena in Natural Sciences*, Springer Series in Synergetics (Springer, Berlin, ed. 2, 2006).
38. A. Clauset, C. R. Shalizi, M. E. J. Newman, Power-law distributions in empirical data. *SIAM Rev.* **51**, 661 (2009). doi:10.1137/070710111
39. M. P. H. Stumpf, M. A. Porter, Critical truths about power laws. *Science* **335**, 665 (2012). doi:10.1126/science.1216142 Medline
40. P. Nelson, Transport of torsional stress in DNA. *Proc. Natl. Acad. Sci. U.S.A.* **96**, 14342 (1999). doi:10.1073/pnas.96.25.14342 Medline
41. C. Levinthal, H. R. Crane, On the unwinding of DNA. *Proc. Natl. Acad. Sci. U.S.A.* **42**, 436 (1956). doi:10.1073/pnas.42.7.436 Medline

Acknowledgments: We thank M. Emanuel and H. Schiessel for discussions on plectoneme energetics, I. De Vlaminck for discussions, D. van der Vlies for experimental assistance, S. Hage and B. Cross for DNA constructs, and J. van der Does for mechanical modifications to the magnetic tweezers. This work has been supported in part by the ERC research grant NanoforBio (#247072).

Supplementary Materials

www.sciencemag.org/cgi/content/full/science.1225810/DC1
Materials and Methods
Supplementary Text S1 to S8
Figs. S1 to S11
Table S1
References (*26*–*41*)
Movies S1 and S2

8 June 2012; accepted 7 August 2012
Published online 13 September 2012
10.1126/science.1225810